

A transient mesophase on drawing polymers based on polyethylene terephthalate (PET) and polyethylene naphthoate (PEN)

G. E. WELSH

Department of Materials Science and Metallurgy, Pembroke Street, Cambridge, CB2 3QZ, UK

D. J. BLUNDELL*

ICI, P.O. Box 90, Wilton, Middlesbrough, Cleveland, TS90 8JE, UK

A. H. WINDLE

Department of Materials Science and Metallurgy, Pembroke Street, Cambridge, CB2 3QZ, UK

E-mail: ahw1@cus.cam.ac.uk

This paper is centred around the identification of a transient mesophase during the drawing of PET and PEN and their associated random copolymers. While the observation of the mesophase has previously been announced as a note (*Macromolecules*, **31**, 1998, p. 7562), this paper sets out the work in appropriate detail. Samples across the full random copolymer composition range are hot drawn, and, either immediately quenched or examined *in-situ* using synchrotron radiation. In each case a mesophase has been observed under drawing conditions which produced little or no crystallinity. That the phase was not the product of the quench was confirmed by the high temperature dynamic measurements. The signature of the mesophase is a sharp, meridional peak in the WAXS fibre diagram which shows no other sharp peaks suggesting crystallinity; the equatorial maxima, while equiaxial and indicating a high level of chain orientation, are diffuse. The mesophase is thus classified as smectic A. SAXS measurements on quenched samples, give no indication that the mesophase is associated with a particular microstructure. The mesophase is seen across the PET/PEN composition range, its observation being more straightforward in the random copolymers where the rate of crystallisation is significantly reduced. Subsequent crystallisation of the fibres by suitable annealing, replaces the meridional mesophase peak on the first layer line with off-meridional crystal reflections characteristic of the triclinic unit cell. The layer line is at a slightly lower angle after crystallisation indicating a longer axial repeat in the crystal than in the mesophase. The development of crystallinity gives rise to a distinct SAXS pattern indicative of a two phase microstructure. The transition from smectic A mesophase to triclinic crystal provides a rationale for the occurrence of oblique lamellae in PET, and associated random copolymers with more than 70% ethylene terephthalate units, as indicated by the four point SAXS patterns, and also for the *c* axis tilt observed in the WAXS patterns. Similarly, for the PEN rich copolymers, the absence of obliquity and consequent *c*-axis tilt, coupled with the marked layer line streaking of the triclinic reflections, can be rationalised in terms of the *c*-shear of the transition being compensated by faulting in the crystal. © 2000 Kluwer Academic Publishers

1. Introduction

Uniaxially deformed fibres and films of poly(ethylene terephthalate) (PET) or poly(ethylene naphthoate) (PEN) produced under normal processing conditions usually contain three dimensional ordered crystalline phases in which the polymer chain axes are closely aligned along the principal deformation axis. However under certain preparation conditions mesophases of intermediate order have been observed in these ho-

mopolymers. In a recent note [1] we announced the observation of a transient smectic mesophase, as observed in both quenched samples and during drawing using synchrotron experiments, which occurs as a precursor of strain induced crystallization in PET, PEN and their copolymers. Further aspects of the results concerning the stability of the mesophase are reported in a following paper [2]. In the present paper we analyse the diffraction from the mesophase, already announced, in

* Present Address: Department of Physics, Keele University, Staffs, ST5 5BG, UK.

more detail. We also focus attention on the relation of the mesophase to the texture of crystals formed during subsequent crystallisation.

Comparatively recently, Keller underlined the thermodynamic grounds for mesophases being favoured as an intermediate step in the crystallization of polymers [3]. The current general interest in such mesophases covers a range of polymers [4–8], and provides a current context to the work on oriented PET/PEN reported here. For example, in unoriented PET, Imai *et al.* [4] have presented clear evidence from SAXS of density fluctuations developing via a spinodal process which they have interpreted as precursors to the crystal nucleation process. Mahendrasingam *et al.* [5] have also recently reported diffraction evidence of mesophase diffraction in PET while it is being rapidly deformed.

In the oriented state, the study of the structure and stability of the mesophase is often impeded by the rapidity of the formation of the crystalline phase. This difficulty has been partly averted in the present study by suppressing the crystallization rate by using copolymers of PET and PEN. The two monomers have similar extended chain configurations but their length along the chain differ significantly. In principle therefore a comonomer incorporated in a sequence of the other monomer will disrupt the regular repeat along the chain direction. However, it has been shown that in this co-polymer system the crystallites are not necessarily true three dimensional crystals of either of the homopolymers but comprise of an alignment of short random matching comonomer sequences [9, 10]. The appearance of an oriented mesophase in this copolymer system which exhibits this particular crystallization (NPL) behaviour adds further insight into the nature of the observed mesophase and its potential role as a precursor to crystallization. Of special interest in this respect is the influence the mesophase has on the chain tilt or internal disorder of the subsequent crystals. The co-crystallization behaviour involving matching alignment of comonomers is analogous to that seen in thermotropic liquid crystalline polyesters (eg random copolymers of hydroxy benzoic and naphthoic acids). It is significant that the molten state of these liquid crystal polymers also exhibits a meridional reflection indicating a smectic mesophase structure [11], which can influence crystal formation on subsequent cooling.

This study is based on copolymers covering the full range of compositions enabling the effects of comonomers on the two extreme homopolymer behaviours to be explored. It involves WAXS and SAXS observation on fibre samples that have been hot drawn, followed by immediate quenching. This work is supplemented by real time WAXS observation of fast drawn film samples using a synchrotron radiation source.

2. Background

2.1. Observation of mesophase structures in oriented PET and PEN

Our observation of transient mesophases across the composition range of the PET/PEN random copolymer system, announced in [1] and reported in fuller detail

here, must be set in a context of several previous reports of mesophases in each of the homopolymers; in PET and, to a lesser extent, in PEN.

Mesophases have previously been reported in both PET and PEN homopolymer fibres prepared in various ways. Bonart [12] prepared a series of ‘paracrystalline mesophases’ by stretching amorphous PET under unspecified conditions. These showed a nematic structure which was transformed to a smectic structure on further stretching. Bonart suggested that these mesophase states characterized the crystallization process of PET, and that features due to nematic, smectic and triclinic crystal packing could all be seen in fibre diffraction patterns from, for example, PET drawn at 90°C. Further work by Bonart [13] indicated that by cold drawing PET at various speeds samples could be produced which gave diffraction patterns with either only diffuse equatorial peaks, indicating a nematic structure, or by drawing at higher speeds, with diffuse equatorials and some distinct meridional reflections, indicating a smectic structure.

Asano and Seto [14] prepared some PET fibres by cold drawing and annealing at 40°C; these fibres gave a similar diffraction pattern to that of the smectic phase reported by Bonart. The diffraction pattern from these fibres consisted of diffuse equatorial reflections and relatively sharp meridional peaks, arising from a layer spacing of 1.03 nm. This spacing is smaller than the repeat of PET in a triclinic crystal (1.075 nm), and indicated that the PET chains were not in a fully extended conformation. Annealing the cold drawn PET above T_g led to the usual triclinic structure. Asano *et al.* [15] have recently reported a further study of the annealing of oriented amorphous PET in which an initial nematic type order is transformed into smectic order during annealing.

Auriemma *et al.* [16] attempted to model the structure of the PET mesophase. A sample was prepared by drawing PET at room temperature and annealing at 60°C; these gave a diffraction pattern with three well defined meridional peaks at 0.96 nm^{-1} , 2.9 nm^{-1} , and 4.8 nm^{-1} , and a broad peak on the equator. Energy minimisation on PET monomer units revealed nine minimum energy conformations, which could be characterized by nearly all-trans conformations except for the CO-O-C-C dihedral angles which could have values close to $180^\circ \sim +80^\circ$ and -80° . Fig. 1 shows PET monomers with the CO-O-C-C dihedral angles at $+80^\circ$ and -80° , a conformation found by Auriemma *et al.* [16] to have a length of 1.04 nm, very close to the PET mesophase repeat length. A model consisting of a regular isolated chain in this conformation which gave a diffraction pattern with strong diffuse layer lines was rejected as a model for the structure of the mesophase, for the intensity

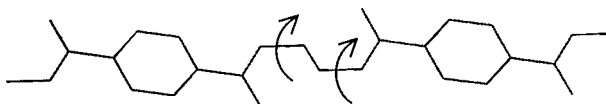


Figure 1 Two PET units with the CO-O-C-C dihedral angles (marked by arrows) set close to $\pm 80^\circ$.

in experimental PET mesophase diffraction patterns is concentrated onto the meridian. Diffraction patterns were then calculated from models of isolated extended linear chains consisting of random sequences of monomer units in different minimum energy conformations, with no correlation between the planes of the phenylene rings along the chains. The simulated patterns showed meridional maxima in the correct positions, but because of a reported ‘absence of layer lines off the meridian’ Auriemma *et al.* [16] concluded that the observed PET mesophase pattern could be qualitatively accounted for by a model of isolated chains with monomer units in random minimum energy conformations. Nicholson *et al.* [17] also performed energy minimization on PET monomer units and found energy minima with the CO-O-C-C dihedral angles close to 80°.

More recently, Jakeways *et al.* [18] reported a mesophase in PEN fibres prepared by spinning at a wind up speed of 500 mm/min followed by drawing at 120° C. These fibres gave diffraction patterns with a series of relatively sharp meridional peaks, and diffuse equatorial peaks. In a further study of this mesophase by Carr *et al.* [19], it was reported that low temperature and high strain rate encouraged mesophase formation. However they found that the mesophase was not very stable and that it could be removed by annealing. They interpreted the fibre diffraction patterns from the PEN mesophase as being from a nematic structure in which substantial lengths of individual chains are fully extended but do not pack laterally in crystalline register. It was envisaged that there was random conformational disorder along the PEN chains.

Mahendrasingam *et al.* [5] have recently reported evidence for a transient mesophase structure in PET during real time fast drawing synchrotron experiments similar to those carried out on PEN and the PEN/PET copolymers [1] and reported in detail here. A faint meridional reflection consistent with a smectic mesophase was seen during the last stages of drawing and was then seen to decay on a similar timescale to the appearance of diffraction from a crystalline phase, implying that the mesophase structures had transformed into crystals.

2.2. Crystal structures of PET/PEN copolymers

The principles of enabling crystallization in random copolymers by sequence matching has been explored in detail in studies of liquid crystal polyesters such as poly(HNA-HBA). This copolymer system can be regarded as an all-aromatic analogue of PEN/PET copolymers. Conventional concepts of crystallization in copolymers envisage a segregated exclusion of monomers to enable the formation of crystals essentially comprising one monomer species. Such concepts cannot explain the high levels of crystalline type order found in HNA-HBA copolymers. Fibre patterns of well crystallised HNA-HBA samples show discrete diffraction sampling on aperiodic layer lines with the first layer line equivalent to a the mean spacing of the monomer composition. Two main models have been proposed

to account for the aperiodic pattern. The non-periodic layer (NPL) model, e.g. Hanna and Windle [20] is based on lateral matching between short but identical random sequences of monomers on neighbouring chains involving crystallographic register. An alternate model of Blackwell and Biswas [21] proposed a “plane start” concept in which random sequences are positioned and held in register only on one single plane perpendicular to the chains. It is difficult to distinguish between models on diffraction evidence alone since both account for discrete sampling on aperiodic layer lines, although further studies by Welsh and Windle [22] suggest that a crystalline region based on many short sequence matches with faults in between, is particularly consistent with the experimental evidence. Later studies of the melt state of the HNA-HBA copolymers revealed a diffraction pattern associated with a smectic mesophase [11] which could be interpreted as a random sequence matching of neighbouring chains but without lateral crystallographic register in the packing of the chains. The presence of a smectic order in the melt helps explain the rapidity with which crystallographic register can occur on cooling to the solid state. However, in the case of this (HBA-HNA) system it should be noted that the sequence matching which aligned the chemical repeats in layers normal to the chain axes was the same as that in the orthorhombic crystal structure which formed on cooling.

The studies of Lu and Windle [9,10] on highly crystalline fibres of PEN/PET copolymers have demonstrated fibre patterns with sampling on aperiodic layer lines across the whole composition range. They have shown that the patterns can be accounted for with an NPL, sequence-matched crystal in which the matching planes are parallel to the *a-b* plane of a triclinic crystal rather than planes perpendicular to the chains. The position of the first layer line varies with composition and is related to the mean period of the monomers in a crystallographic conformation. Lu and Windle also showed that the triclinic cell also varies with composition and is either based on the cells of PET or PEN depending on the predominant comonomer, the transition occurring at about 70% PEN. When the PET cell is adopted, the patterns show a systematic displacement of reflections above and below the layer lines. This feature indicates a significant tilt of the chain axis with respect to the to the fibre axis. When the PEN cell is adopted, the reflections are closely aligned onto the layer lines, but tend to show a ‘streaking’ along the layer lines.

3. Experimental

3.1. Sample preparation

Amorphous monofilaments of random copolymers were drawn by hand in a silicone oil bath at a rate of approximately 2 s⁻¹. Most of the samples were cooled rapidly by quenching into iced water; these will be referred to as quenched samples. Draw ratios were measured by marking the monofilaments with ink stripes separated by 5 mm; the stripe separation after drawing was measured and averaged for all samples in a batch prepared under the same conditions. The draw ratios

did not vary by more than 10% within a batch of samples, and were reproducible in other batches of samples prepared in the same way. When drawing samples by hand there is a maximum draw ratio at which the fibres become suddenly too stiff for further elongation. For 50% T/N the maximum draw ratio is about 10, so it is possible to draw samples to half this draw ratio. The maximum draw ratio for PET and PEN rich samples is only about 5, but the samples can be quenched before strain hardening is detected.

The advantages of hand drawing is the speed with which the samples can be quenched under load, the transfer time from oil to iced water being of the order of 100 ms. The oil bath also provides a very accurate control of draw temperature ($\pm 0.1^\circ\text{C}$).

3.2. Wide angle X-ray scattering

Wide angle X-ray fibre diffraction patterns were obtained from bundles of fibres using beamline 7.2 at the Synchrotron Radiation Source at Daresbury with a wavelength of 0.1488 nm. The patterns were collected on MAR image plates and were quadrant averaged and mapped into reciprocal space using the CCP 13 software, which uses the methods of Fraser *et al.* [23]. Diffractometer scans were performed on rafts of parallel fibres, using a Siemens D500 diffractometer in transmission mode. Ni filtered Cu K_α radiation was used, with 0.1° divergence and anti-scatter slits, and a 0.15° receiving slit. The samples were calibrated with silicon powder giving peaks at 0.314 nm and 0.192 nm. Data points were collected from $4^\circ 2\theta$ to $50^\circ 2\theta$, at intervals of $0.1^\circ 2\theta$.

Selected samples were also examined by SAXS beamline 2.1 at the Synchrotron Radiation Source using a wavelength of 0.1544 nm. The SAXS patterns were collected with a 2D multiwire detector and analysed using FIT2D software.

3.3. *In situ* hot drawing and wide angle X-ray scattering

The time-resolved *in situ* hot drawing experiments were carried out on the microfocus beamline ID13 at the European Synchrotron Radiation Facility (ESRF), using the same experimental procedure recently used in the study of fast drawn PET [24, 25]. The experiments made use of a purpose designed, X-ray diffraction camera constructed at the University of Keele [26]. The camera consisted of an oven with a viewing port in which a video camera was mounted. The oven temperature could be controlled to within 1°C . Samples cut from polymer films were clamped between two jaws attached to stepper motors which allowed uniaxial drawing.

The microfocus beamline had a highly collimated beam with a diameter of approximately $30\ \mu\text{m}$ at the specimen, with a wavelength of 0.092 nm. A minimum specimen to detector distance of 60 mm was available, at which d spacings out to 0.15 nm could be recorded. A continuous series of diffraction frames were recorded

using a Photonics Science CCD detector, with an exposure time of 40 milliseconds for each frame. 124 frames were recorded sequentially, with essentially no dead time between frames. The variation in size and shape of the specimen during drawing was recorded by the video recorder, also as a series of 40 millisecond frames. The collection of the video recorder and X-ray diffraction frames was synchronized.

The experiments were carried out on amorphous 50% T/N films, $810\ \mu\text{m}$ thick which were obtained by melt pressing at 170°C ; amorphous cast PEN films $520\ \mu\text{m}$ thick were provided by W. A. MacDonald (Dupont Polyester Films). 10 mm wide samples cut from the amorphous films were used. Ink reference stripes were drawn onto the films with a separation of 1 mm right angles to the draw direction, to allow the draw ratio to be calculated from the video camera images. The samples were mounted in the jaws of the camera with a 10 mm gauge length. A nominal draw rate of $12\ \text{s}^{-1}$ was used for all the samples although during the deformation of a neck the local draw rate differed from this. The 50% T/N sample was drawn at 120°C ; PEN samples were drawn at 130°C and 150°C .

4. Results

4.1. 50% T/N mesophase WAXS diffraction patterns

Fig. 2 shows examples of fibre diffraction patterns from 50% T/N fibres which have been drawn at 100°C , a) to a draw ratio (DR) of 6 and ice quenched, b) to DR 10 and ice quenched, c) to DR 10 and air cooled and, for comparison, d) to DR 10, air cooled and annealed at constant length at 100°C for 24 h; inset boxes show expanded views of the first meridional reflections. The three patterns from unannealed fibres all show a sharp and intense low angle meridional reflection at $0.86\ \text{nm}^{-1}$, and a broader high angle meridional reflection at $4.8\ \text{nm}^{-1}$. Only the edge of the high angle meridional peak can be seen because of the curvature of the Ewald sphere.

The main equatorial feature on these patterns is a diffuse peak at about $0.4\ \text{nm}$ although in patterns b) and c) crystal peaks are superposed upon it. Fig. 3 shows equatorial scans taken from the fibre diffraction patterns of Fig. 2 by vertically integrating the first twelve rasters of each averaged quadrant of the patterns. The sample which had been drawn to DR 6 has no crystal component, whilst those drawn to DR 10 have started to crystallize. The annealed sample, Figs 2d and 3d, has sharp crystalline peaks from a non periodic triclinic structure. Significantly, there is no sharp meridional reflection in the region of $0.86\ \text{nm}^{-1}$ in its fibre diffraction pattern. Annealing, again at 100°C and 24 hours, the sample drawn to DR 6 and ice quenched (diffraction pattern 2 a), resulted in crystallization and, as with the DR 10 sample, in the loss of the low angle meridional peak.

A pattern indistinguishable from Fig. 2a was obtained from a 50% T/N fibre drawn to DR 6 at 120°C , instead of 100°C , and ice quenched. However, drawing at 110°C gave fibres whose diffraction patterns showed

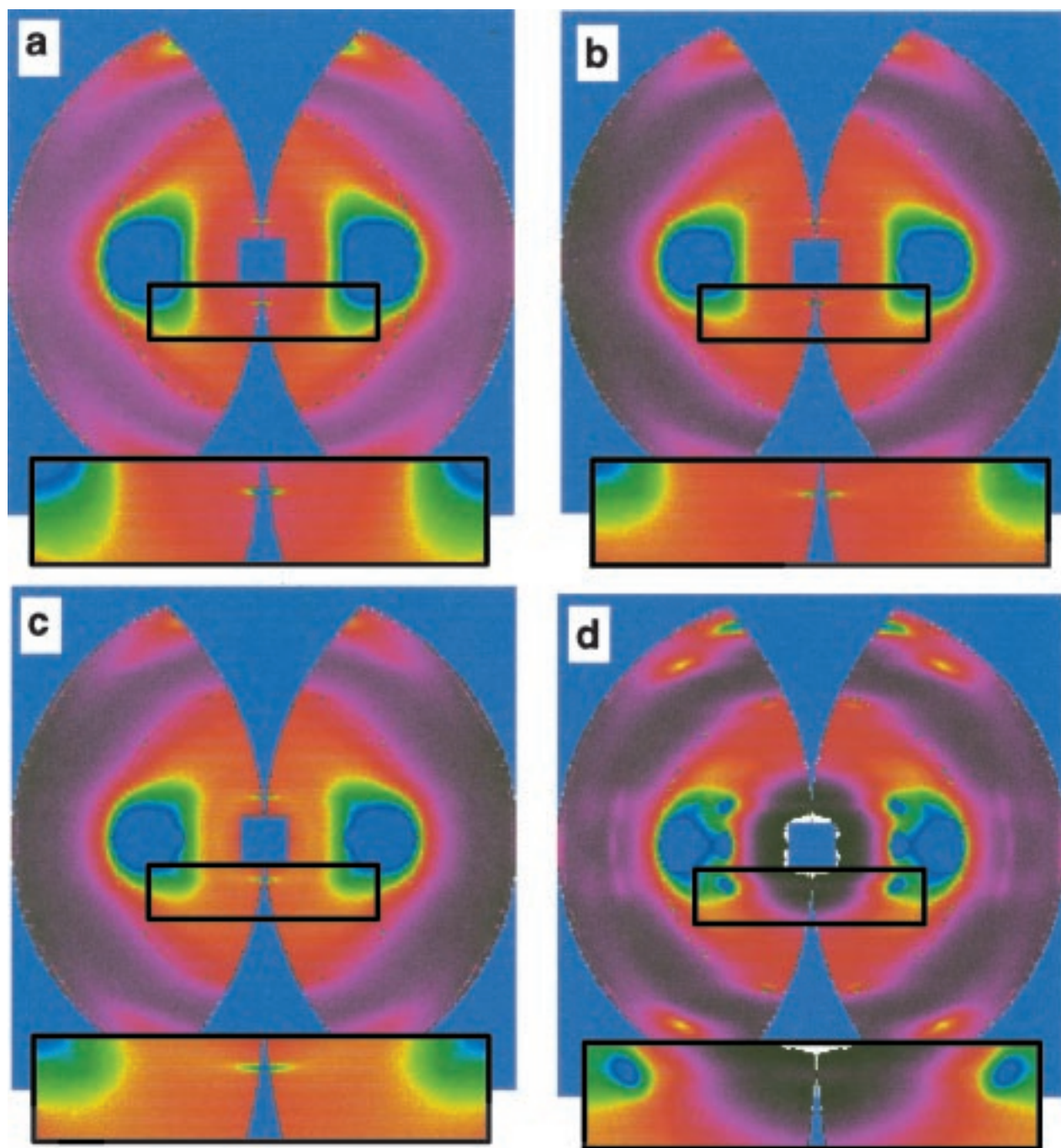


Figure 2 Wide angle x-ray diffraction patterns from 50% T/N fibres drawn at 100°C. (a) drawn to DR 10 and quenched into iced water; (b) drawn to DR 10 and quenched into iced water; (c) drawn to DR 10 and air cooled; (d) drawn to DR 10 air cooled and annealed at 100°C for 24 h. The diffraction patterns have been mapped onto a planar section of reciprocal space and quadrant averaged, the blank region about the meridian is inaccessible due to the curvature of the Ewald sphere. The fibre axis is vertical and the patterns extend to 5.2 nm^{-1} . The inset is a magnification of the marked region containing the first meridional reflection.

crystalline peaks, superposed upon a mesophase pattern, similar to Fig. 2c; it appears that at this intermediate temperature 50% T/N fibres crystallize too fast to enable a pure mesophase state to be caught by quenching.

4.2. Real time WAXS diffraction from 50/50 copolymer

Fig. 4 shows series of diffraction patterns from an amorphous 50% T/N film recorded during hot drawing at 120°C. Fig. 5 shows the corresponding video images of the film as it was stretched. The initial diffraction

pattern shows no sign of orientation, but by the 4th frame the intensity of the main diffraction halo has started to become concentrated onto the equator. The concentration of intensity onto the equator becomes more marked in the 5th frame, this corresponds to a draw ratio of about 3 in the necked region that was being penetrated by the microbeam. There are no sharp reflections in the frame 5 diffraction pattern, the broad equatorial peaks indicate a structure in which there are highly oriented parallel chain segments packed laterally in a liquid like manner.

A distinct, albeit faint, meridional reflection first become visible in the frame 6 diffraction pattern. Fig. 6

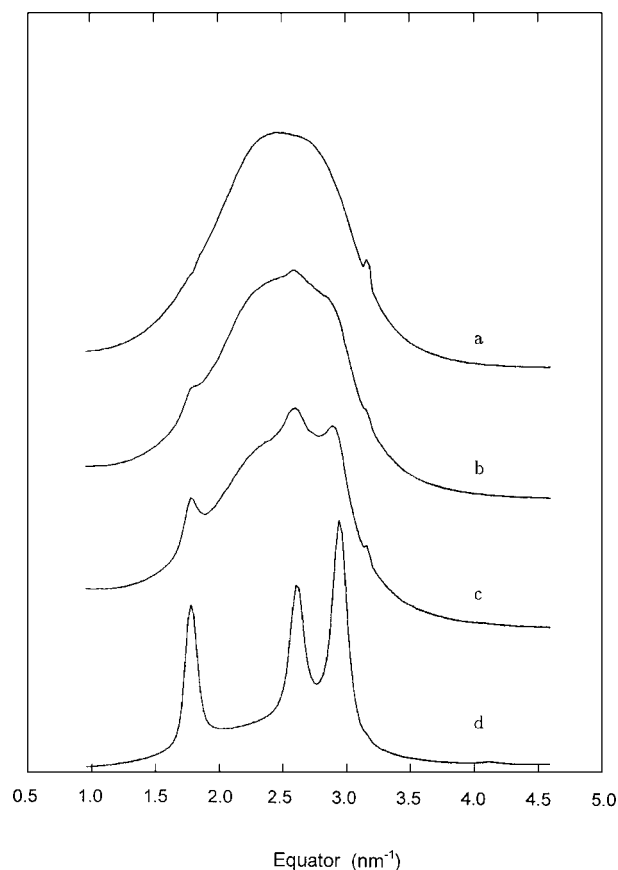


Figure 3 Equatorial scans from the diffraction patterns of Fig. 2a–d. The vertical axis is intensity in arbitrary units.

shows an expanded view of the frame 7 diffraction pattern, in which meridional reflections can be seen clearly; there is a very sharp meridional at the lower, and a broader meridional at a higher angle. It should be remembered that due to the curvature of the Ewald sphere, the meridian cannot be accessed completely, and the high angle peak is only the edge of a reflection which has been spread out, probably by disorientation. The pattern in frame 7 is very similar to the diffraction pattern obtained from 50% T/N fibres which have been extended to DR 6 and quenched before crystallization could occur (see Fig. 2a). The sharp low angle meridional reflection and broad equatorial peak, indicate that the polymers are arranged in liquid crystal like packing, with some axial register between neighbouring chains, but with liquid like lateral packing of polymer chains.

Although the mechanical movement of the crossheads ceased during frame 6, the part of the sample in the X-ray beam continued to draw and thin down at the same deformation rate to reach a draw ratio of 9:1 at frame 11. During this period there was both a significant intensification of the meridional reflection and an increase in prominence of the diffuse scatter at the equator. After frame 11 and for the remainder of the experiment, the local deformation rate then slowed down to reach a draw ratio of about 13:1 in the final frame 124. Between frame 11 and 124 there is a measurable reduction in the intensity of the sharp meridional reflection relative to the overall scattered intensity and there is also a reduction in the diffuse intensity concentrated on the equator.

The changes in this last stage of the experimental observation indicate a gradual reduction in the number of extended, oriented chains with a corresponding loss of axial register between them. A more detailed analysis of the quantitative changes during the growth and decay of the meridional reflection is reported separately [2].

During the 5 seconds of the recorded diffraction of this experiment, no crystalline reflections were detected. It is possible that the sample did not crystallize during this timescale because it was being drawn quite close to its melting point ($T_m = 135^\circ\text{C}$ for 50% T/N). However a diffraction pattern collected from this sample after it had been removed from the drawing rig and allowed to cool down showed three strong Bragg peaks on the equator, indicating that the sample had crystallized after the experimental recording had ceased and possibly during the subsequent cooling of the sample.

During the corresponding drawing experiments on PEN, the crystallization process was too rapid to resolve the exact sequence of structural changes at the start of the crystallization processes. However the meridional reflection associated with the mesophase was visible for a few frames during the initial stages of the crystallization near the end of the draw and then diminished as the crystallization proceeded. Although no frame shows solely the mesophase reflection without any accompanying crystalline reflections, the sequence of events is consistent with the similar time resolved experiments on PET where the mesophase was observed as a precursor to crystallization [5].

4.3. Mesophase diffraction patterns across the composition range

Fig. 7 shows diffraction patterns from quenched samples of a) 84/16% T/N, b) PET, c) 16/84% T/N and d) PEN. In each case the draw ratio was 5 and the samples were quenched into iced water. The draw temperatures were, a) 90°C , b) 120°C , c) 75°C and d) 120°C . As in Fig. 2, the inset boxes show an expanded view of the first meridional peaks. A broad and diffuse equatorial reflection, a sharp meridional reflection at low angle; and broader meridional reflections at higher angle, are visible on all the patterns. The PEN rich samples have clearly started to crystallize as Bragg peaks are visible on the equator of some of the layer lines.

Most of the information in diffraction patterns from PET/PEN quenched fibres lies on the meridian. Fig. 8 shows meridional diffractometer scans from quenched fibres of Fig. 7 with the addition of that from Fig 2a (D.R. = 6 and iced water quench). Strong peaks can be seen corresponding to the first layer line mesophase peaks on the fibre diffraction patterns. Other peaks are also visible on the diffractometer scans, all the peak positions are tabulated in Table I. This table also gives the ideal reflection positions calculated on the basis of the highest order observed meridional peak (a fifth order peak for PET and a sixth order peak for PEN), which should give the most accurate value of the repeat. Differences between the observed and ideal peak positions will be discussed below.

Fig. 9 shows an expanded view of the meridional diffractometer scans in the region of the first peak.

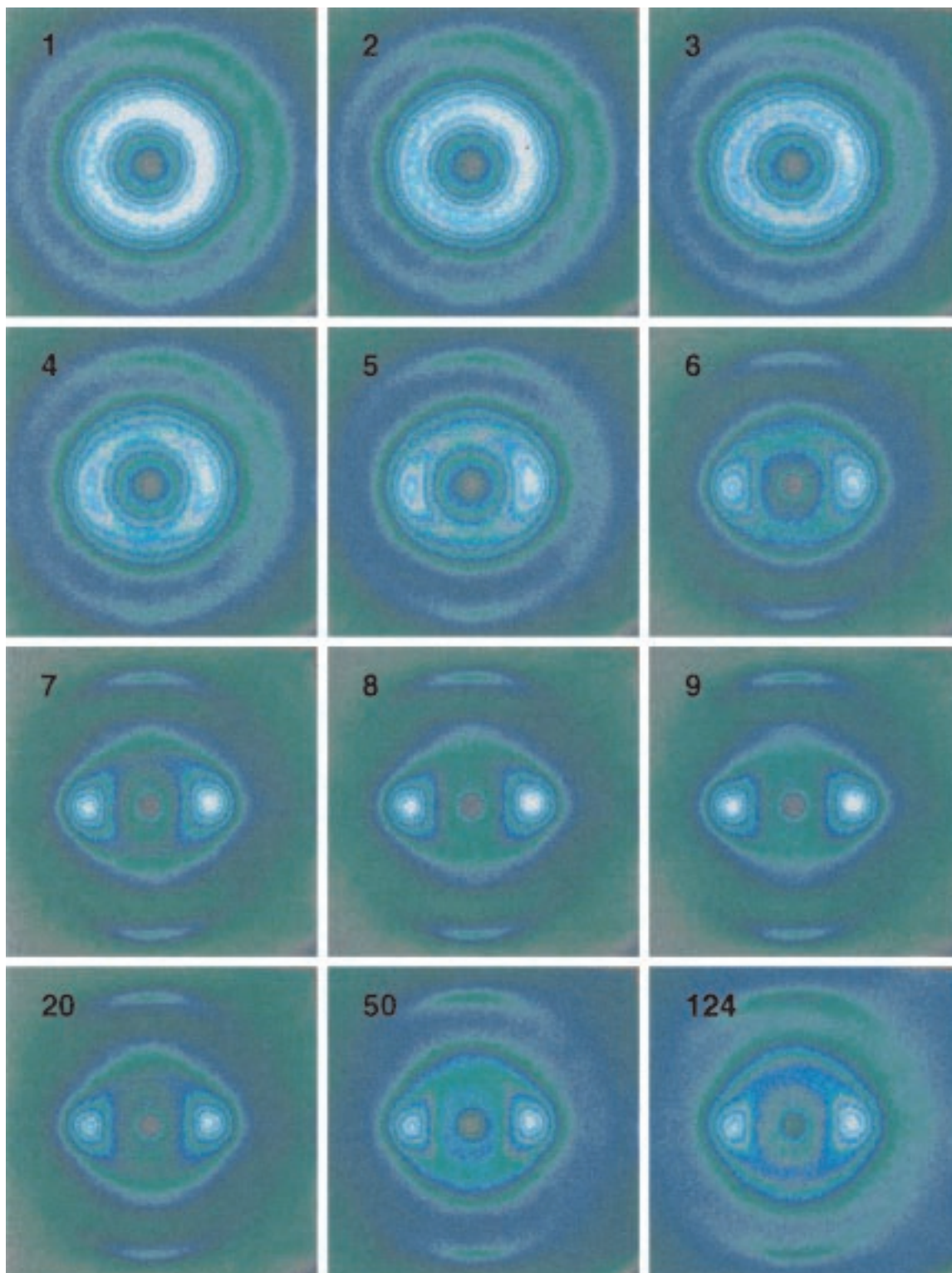


Figure 4 A sequence of wide angle diffraction patterns taken during the drawing of 50% T/N film at 120°C. Each exposure corresponds to a time interval of 40 ms.

Background scattering was subtracted from this region (0.6 nm^{-1} to 1.0 nm^{-1}) by combining the scaled diffractometer data from the PET and PEN scans in the region in which each of these scans has no peak, and subtracting this from each of the diffractometer scans. Removal of the steeply sloping background scattering from the diffractometer scans allowed the peak positions, of the first meridional peaks, to be measured more accurately. The position of the first meridional can be seen to vary with composition in a similar manner to the first layer

line positions from the crystalline random copolymer fibres. Fig. 10 shows an expanded view of the diffractometer scans in the region of the high resolution 5th/6th order peaks; like the corresponding layer lines in crystalline PET/PEN random copolymer fibre diffraction patterns, these peaks move very little with change in composition. It is clear that the mesophase patterns have non-periodic layer lines.

Fig. 11 shows a plot of the chain repeat distance corresponding to the first meridional maximum; the chain

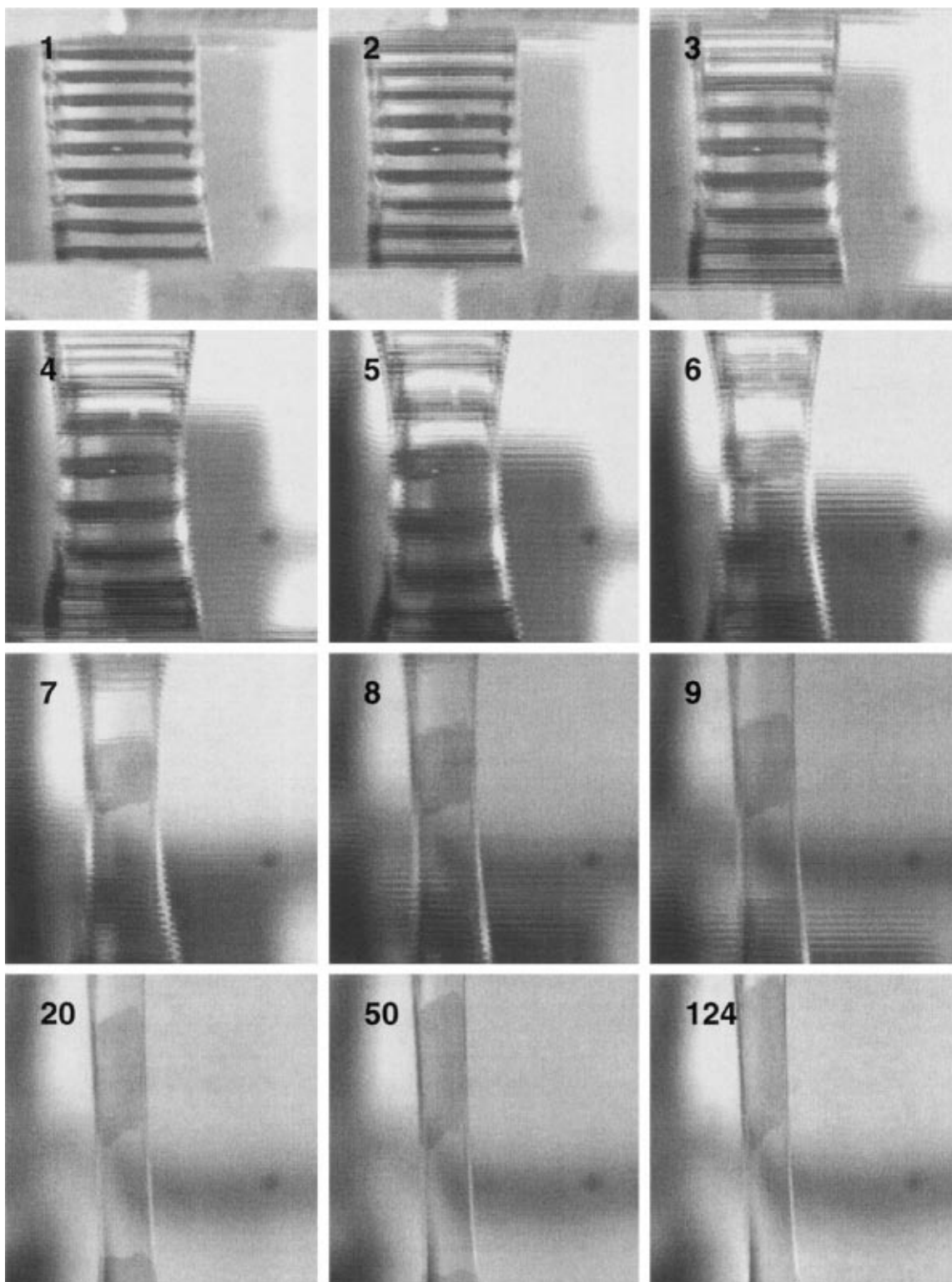


Figure 5 A sequence of video frames showing the deformation of 50% T/N film during uniaxial drawing at 120°C. The frames correspond exactly by number to those of Fig. 4. The draw head motion was stopped during frame 6, although the sample continued to thin in the central shown until frame 20.

repeats obtained from the first layer lines of annealed crystalline fibres are also shown for comparison. The chain repeat for the mesophase samples varies with composition in the manner characteristic of random copolymers in which co-crystallization is occurring, at least in the mid-range compositions. At all compositions the axial repeat in the mesophase is smaller than that measured from annealed samples. The difference is greatest for the samples rich in PEN, where the chain repeat is reduced by about 5% from its length in the

crystalline samples; in PET rich samples this reduction in length is about 3% of the fully extended monomer repeat distance which is in good agreement with Asano and Seto [14].

SAXS patterns are shown in Fig. 12 for samples prepared under the conditions that give the WAXS patterns, a), c) and d) shown in Fig. 7, namely draw to DR = 5 and quench. In the quenched samples showing the mesophase reflection but no significant crystalline reflections, the SAXS patterns are isotropic, despite

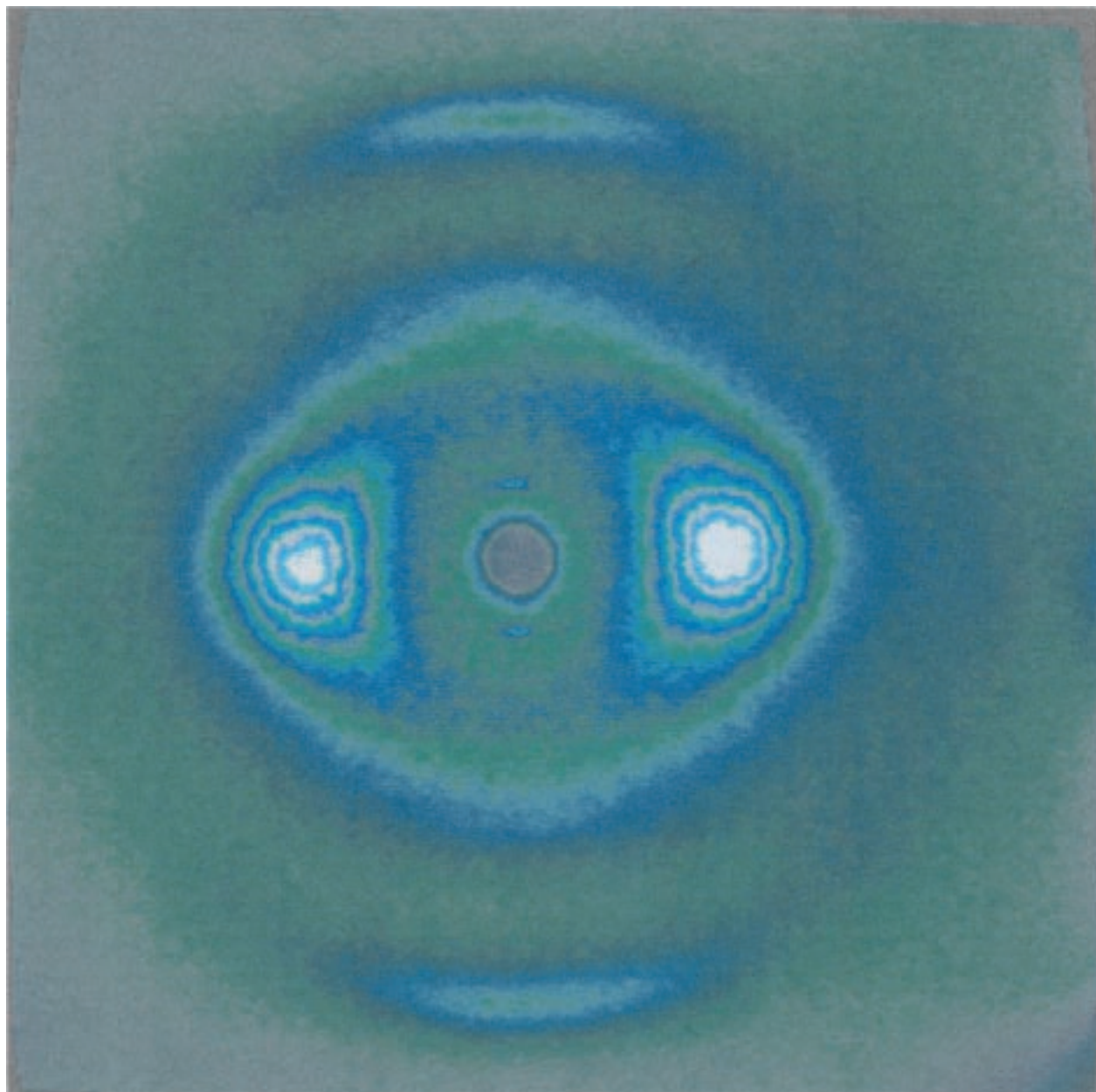


Figure 6 An enlargement of frame 7 of Fig. 6 in which the sharp meridional reflection is first clearly visible.

high chain orientation indicated by WAXS. The intensity is low and does not show any maximum suggesting there is either no separation into discrete mesophase and amorphous regions, or that there is no significant density difference between these regions. According to the Scherrer equation, the width in the Z direction,

of the first meridional reflection in the mesophase fibre patterns corresponds to an axial crystallite size of 20 nm or more; this could mean that the fibres consist predominantly of highly oriented polymer chains, and there is no two-phase microstructure. Alternatively, it is possible that such a microstructure does exist yet, the density difference between the amorphous and mesophase regions is insufficient to give significant contrast and thus a SAXS signature.

TABLE I Peak positions (in nm^{-1}) from the meridional diffractometer scans of Fig. 8

Peak Order	1	2	3	4	5	
PET	0.96	1.94	2.91	—	4.76	
84/16% T/N	0.94	1.85	2.91	—	4.78	
Ideal 1.05 nm repeat	0.95	1.90	2.86	3.81	4.76	
Peak Order	1	—	—	—	5/6	
50/50% T/N	0.865	—	—	—	4.80	
Peak Order	1	2	3	4	5	6
16/84% T/N	0.815	—	2.32	3.16	3.81	4.78
PEN	0.805	—	2.33	3.18	3.83	4.78
Ideal 1.255 nm repeat	0.797	1.59	2.39	3.19	3.98	4.78

Fig. 13 shows the SAXS of annealed fibres from across the composition range. The WAXS patterns show well developed crystalline patterns without the meridional smectic reflection but the SAXS give strong and anisotropic patterns. The SAXS from compositions in which the structures are based on the PET triclinic cell (70%–100% T/N) show a four point pattern whereas for the samples with structures based on the PEN triclinic cell the SAXS is a two-point pattern. The other major aspect of SAXS of the annealed fibres is that the 50% T/N composition does not show

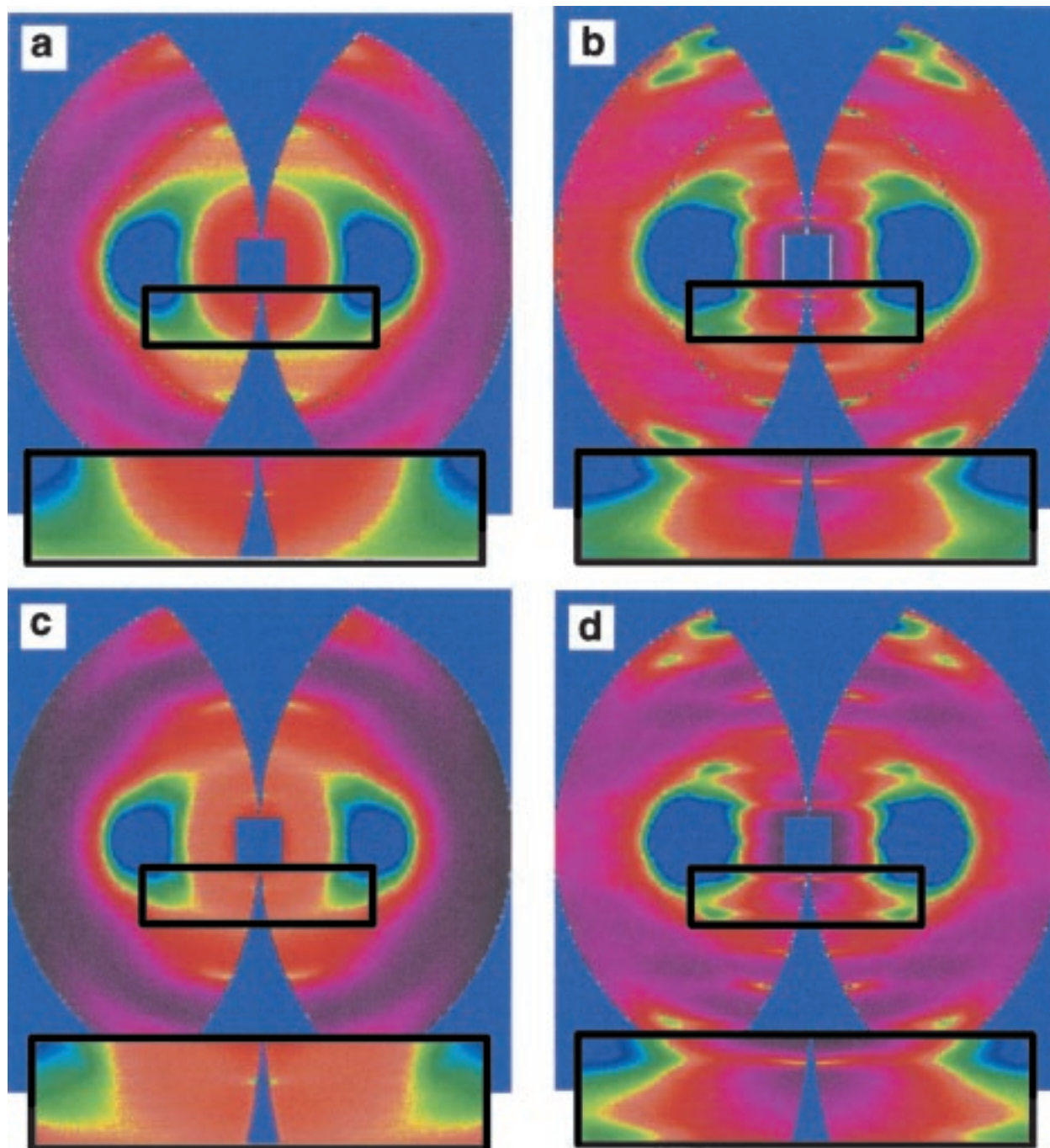


Figure 7 Wide angle fibre diffraction patterns presented in the same way as in Fig. 2. (a) 84/16 T/N, D.R. 5 at 90°C, quenched into iced water. (b) 16/84 T/N, D.R. 5 at 120°C, quenched into iced water. (c) PET, D.R. 5 at 65°C, quenched into iced water. (d) PEN, D.R. 5 at 120°C, quenched into iced water.

any discrete reflections although the scattering is significantly anisotropic. It would appear that the crystals in the 50% sample, and to a lesser extent, those of the 40% and 60% T/N samples, are not sufficiently regularly arranged to give a completely discrete SAXS interference peak. However, a more detailed investigation, almost certainly involving electron microscopy, would be necessary to obtain firm conclusions on this matter.

The long periods measured from the two dimensional SAXS patterns are listed in Table II. It should be noted that the transition from a two point diagram to a four point one as the T content reaches 70% is associated with a discontinuous drop in long period, but little discontinuity of the long period resolved in the axial di-

rection. For the PEN based (2 point SAXS) samples it is interesting to compare the PEN homopolymer with the 50/50 T/N random copolymer. The crystallinities have been estimated at 50% and 30% respectively by Welsh [27], which would imply crystal thicknesses of the order of 7.5 nm for PEN but 6.0 nm for 50/50 fibre (each corresponding to 5–6 monomers thickness) but amorphous region thicknesses of the order of 7.5 nm and 14.0 nm respectively.

5. Discussion

5.1. The structure of the mesophase

The X-ray diffraction patterns from PET/PEN random copolymer monofilaments, which have been quenched

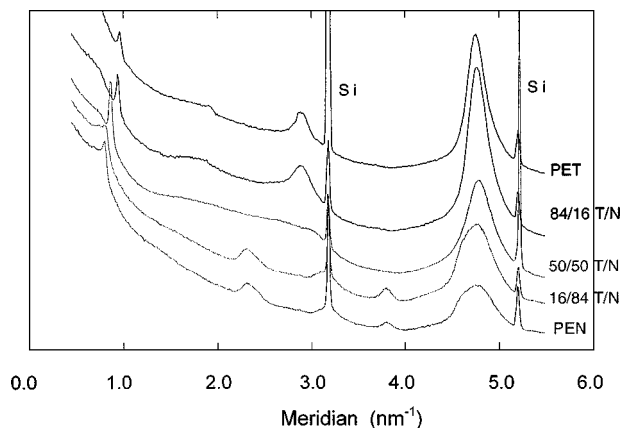


Figure 8 Meridional diffractometer scans from quenched samples. They are from the four fibre patterns of Fig. 7 and from Fig. 2a. The sharp peaks are from silicon powder used as a calibrant and the vertical axis is intensity in arbitrary units.

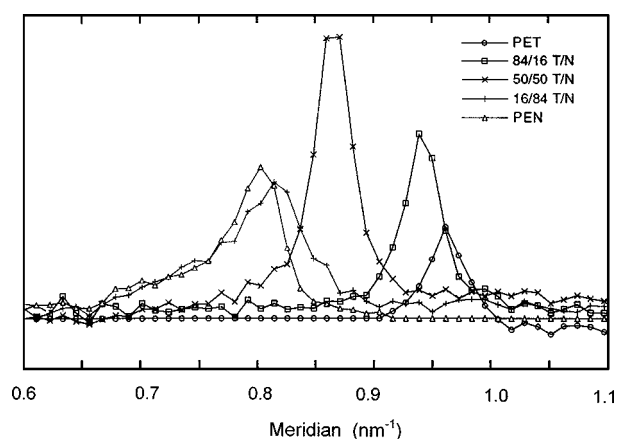


Figure 9 An enlargement of the range 0.6–1.1 nm^{-1} from Fig. 8 to show the positions of the 'mesophase' peak on the first layer line. The steeply sloping background has been subtracted.

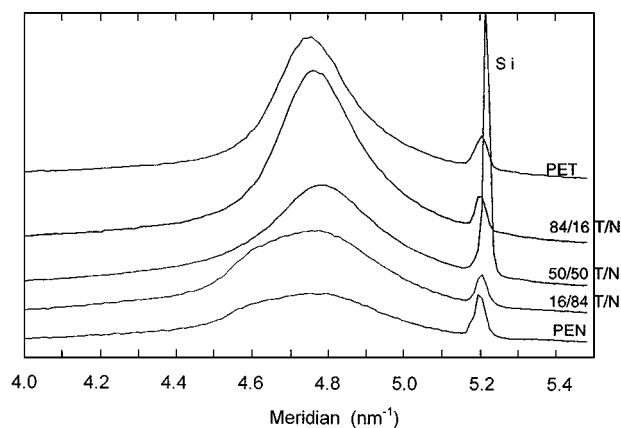


Figure 10 An enlargement of the range 4–5.5 nm^{-1} from Fig. 8. The meridional maximum corresponds to the 5th order from the PET sample, and the 6th order from PEN. The PEN rich samples have a shoulder at around 4.6 nm^{-1} because the samples have started to crystallise.

whilst drawing at temperatures close to T_g , show a mesophase pattern. The mesophase pattern consists of a strong, broad peak on the equator at a spacing corresponding of 0.4 nm, and a series of well defined meridional peaks. At all compositions the first order meridional peak is especially sharp and varies in position with

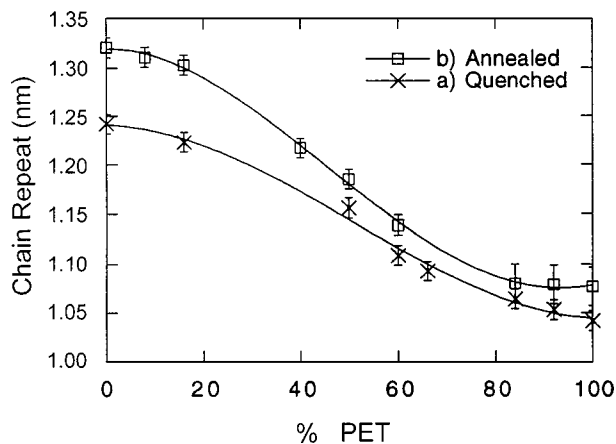


Figure 11 Variation of the chain repeat with composition from the meridional 'mesophase' reflections where these were visible in quenched samples. They are compared with the repeats from the drawn and annealed crystalline samples. In each case the repeats were measured from the first layer line.

composition in a similar way to the first layer line in the crystalline diffraction patterns from the random copolymers; it also has a narrow lateral width concentrated around the meridian. The fifth/sixth order meridional peak is very strong, and varies little in position with changes in composition. In addition, the PET rich samples give a third order meridional peak. This seems to be smeared out and shifted to higher angle on going to 50% T/N. PEN rich samples may give meridional peaks other than the first and fifth order, but it is hard to distinguish these from features arising from the scattering from the crystalline components of the samples. The spacing associated with the meridional peaks is less than the c -axis repeat of the corresponding crystalline state. This indicates that the monomer units in the mesophase are not as fully extended as the fully extended conformation in the crystalline state. However the positions and the appearance of the meridionals are consistent with the aperiodicity associated with extended chains with a random monomer sequence. In this respect the mesophase of the random copolymers echoes the aperiodicity exhibited in the crystalline phase [9].

The patterns are reminiscent of those from the liquid crystalline random copolymers HBA/HNA, particularly those observed by Hanna *et al.* [11] in the sheared melt, where there were sharp meridional peaks but no

TABLE II The long period of annealed fibres across the full composition range. They are measured from 2D SAXS patterns, examples of which are shown in Fig. 13. († indicates increased uncertainty in this measurement as the maximum was not especially obvious)

% PET	Long Period (nm) ± 0.5 nm
0	14.7
8	15.2
16	16.1
40	19.4
50	19.7†
60	19.0
70	13.9
84	13.5
92	12.3
100	11.4

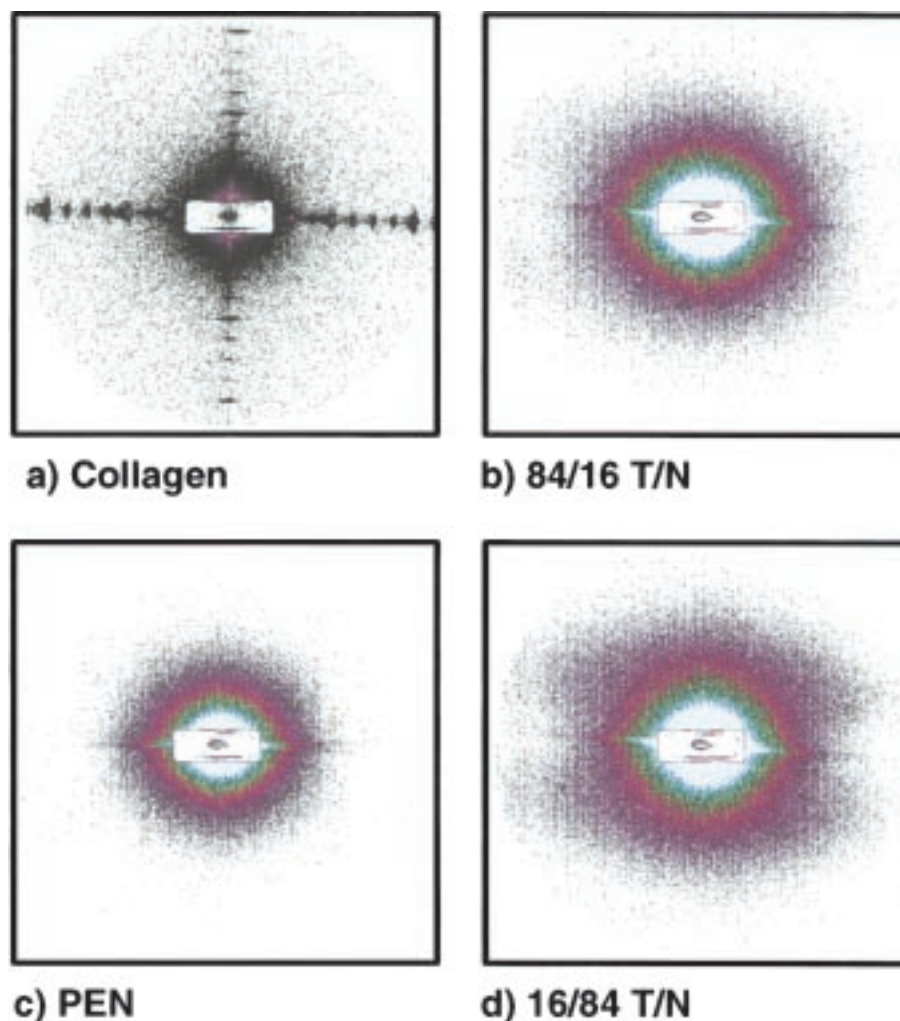


Figure 12 Small Angle X-ray Diffraction (SAXS). (a) Collagen used to calibrate the images patterns (vertical and horizontal patterns superimposed). The strongest peak at the highest angle is 0.135 nm^{-1} (7.4 nm), (b) 84% T/N drawn at 90°C and quenched, (c) PEN drawn at 130°C and quenched and (d) 16% T/N drawn at 130°C and quenched.

Bragg sampling on the equator. The strong but diffuse equatorial peaks in the PET/PEN mesophase patterns indicate the parallel alignment of straight chains, but since there is no Bragg sampling on the equator the chains must be packed laterally in a liquid like manner. The presence of sharp meridional reflections indicates that there is axial register between monomers on adjacent chains, in which the plane of register is perpendicular to the chain direction. This is different to the crystalline structure of these polymers in which the plane of register is on a slant consistent with the triclinic crystal structures. The structure of the mesophase could be classified as smectic A, or ‘chained’ smectic A, as the correlation is between chemical repeat units rather than molecule ends.

While, the patterns from the quenched fibres have key features of a smectic type of order, it is necessary to counter suggestions that the mesophase meridional peak is simply the transform of an isolated molecule, and thus the structure should be classified as nematic. The full width at half height in the R direction (along the layer line) of the first meridional peak is of the order of 0.15 nm^{-1} except in the case of the strongly PEN rich samples where it is larger. The longitudinal register between chains in the mesophase thus extends laterally

over distances of the order of 7.0 nm, or ten chains or more. The first meridional mesophase peak thus cannot be accounted for by the molecular transform of an isolated chain associated with the scattering from parallel but uncorrelated polymer chains [28]. This interpretation, in terms of smectic A organisation is in line with Bonart [12] and a recent paper by Asano *et al.* [12]. It differs from the conclusions of Auriemma *et al.* [16] who proposed that the mesophase structure of PET is essentially nematic, with no axial register between adjacent chains or correlation between the planes of the phenylene rings. It also seems that Carr *et al.* [20] proposed a nematic structure for the PEN mesophase.

5.2. Transient nature of the mesophase

Previous reports of mesophases in PET and PEN, with the exception of Bonart [12], have been of a distinct phase obtained by preparing samples using a particular method, especially drawing at room temperature and annealing below T_g . Diffraction data from the PET and PEN quenched samples obtained here are in good agreement with those reported by Bonart [12], Asano and Seto [14] and Jakeways *et al.* [18]. However, it is proposed here that as well as a phase that can be obtained by certain processing methods, this mesophase is

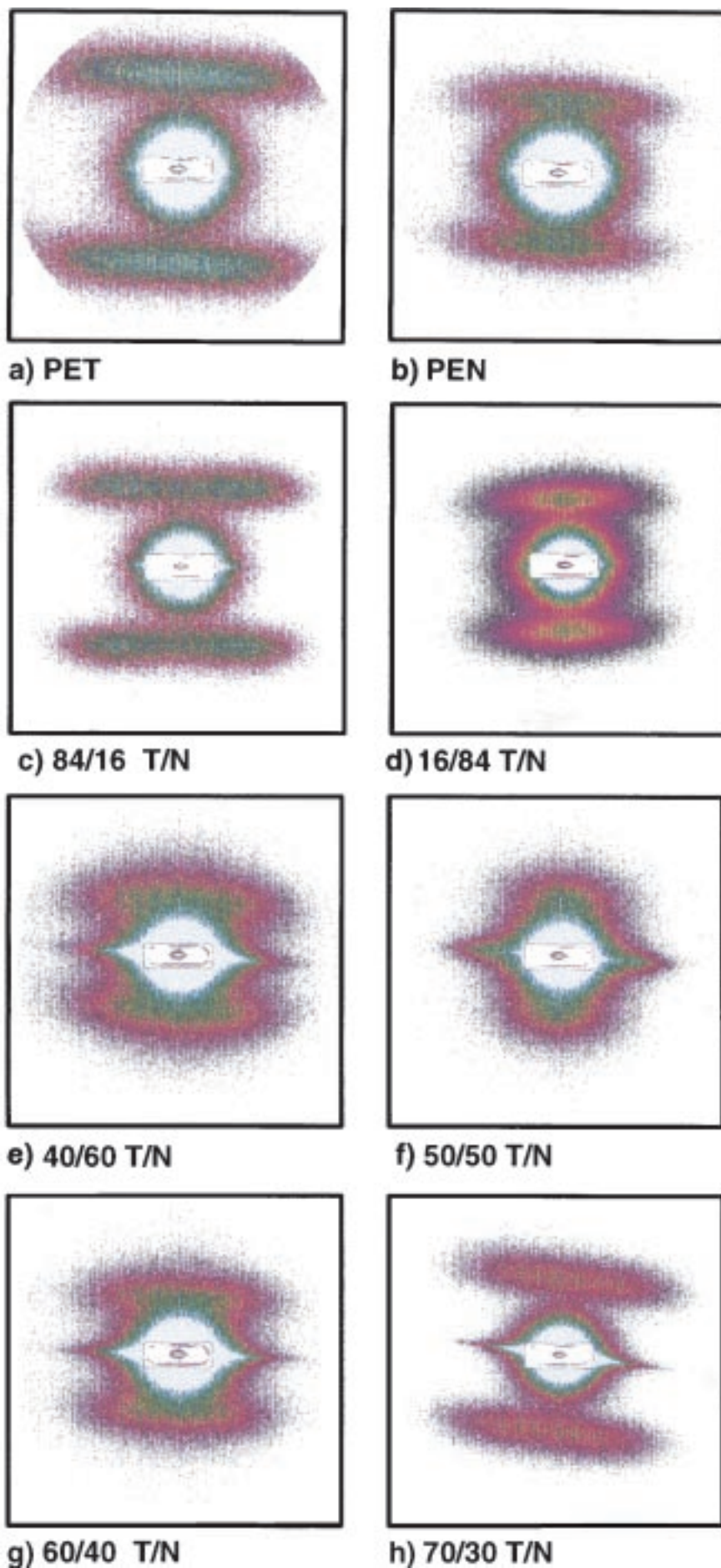


Figure 13 Small angle diagrams corresponding to those of Fig. 12 from samples which have been drawn quenched and annealed for 24 h. (a) PET drawn at 90°C and annealed at 190°C, (b) PEN drawn at 130°C and annealed at 210°C, (c) 84/16 T/N drawn at 90°C and annealed at 190°C, (d) 16/84 T/N drawn at 130°C and annealed at 210°C, (e) 40/60 T/N drawn at 110°C and annealed at 140°C, (f) 50/50 T/N drawn at 110°C and annealed at 115°C, (g) 60/40 T/N drawn at 110°C and annealed at 130°C, (h) 70/30 T/N drawn at 100°C and annealed at 140°C,.

also a transient phase which occurs during hot drawing as a precursor to crystallization.

The WAXS patterns for 50% T/N fibres in Fig. 2 illustrate different degrees of development of crystallinity depending on the drawing and quenching conditions. When the fibre is extended to DR 6 and then quenched there are no signs of crystallinity; only scattering from the mesophase is apparent. Annealing leads to full crystallization and the disappearance of mesophase peaks from the fibre diffraction patterns. This suggests that the mesophase forms before crystallization. When extended to a larger draw ratio of DR 10 and quenched, weak crystal peaks appear in its diffraction pattern, superimposed upon the broad equatorial peaks from the mesophase. It would appear that the mesophase can be at least partly converted into crystalline material as drawing progresses if the deformation is large enough. It could be argued that the first meridional seen in these patterns was formed during cooling and is not representative of the structures formed during the draw. However the data from the time resolved wide angle diffraction/hot drawing experiments provide conclusive evidence that, for 50% T/N at least, the mesophase occurs during the drawing process when a sufficient level of molecular orientation is achieved. The transient appearance of the mesophase in the real time experiment on PEN show that it not only forms during the draw but that it is replaced by crystalline reflections as crystallinity develops. The recent report on similar experiments on PET by Mahendrasingam *et al.* [5] shows a sequence of a mesophase forming and then being replaced by crystals. There is therefore no doubt that at least under certain drawing conditions that a smectic mesophase occurs as a transient intermediate of crystallization.

The transient nature of the smectic mesophase in these PET/PEN copolymers is in contrast to the stable mesophase seen in the HBA/HNA thermotropic liquid crystal copolyesters. In the more rigid chains of the HBA/HNA system it has been shown by Hanna *et al.* [11] that the mesophase forms spontaneously in the melt state and that it can act as a template for rapid crystallization on cooling. In the case of PET, the mesophase only becomes a viable structure in the presence of an externally applied strain field. The decay of the mesophase in the real time 50% T/N experiment illustrates the fragility of the structure when chain relaxation mechanisms remove the local internal stresses [2].

5.3. Crystallization from the mesophase

In the smectic mesophase which forms during hot drawing, longitudinal register between chains occurs in layers which are perpendicular to the chain direction, i.e. smectic A order. On crystallization the register shifts to become triclinic, and the meridional mesophase peak decays as the layer line, or at least one close to it corresponding to a slightly larger axial repeat, is sampled by off meridional crystal reflections. Such a shift in register requires axial staggering of successive chains within a crystallite. Successive staggering would lead to a build up of stress on a crystallite, from the amorphous chains above and below it, which have been made more

taught by the staggering. Consideration of the ways in which this stress might be relieved may be tentatively used to explain some of the features in the wide angle X-ray diffraction patterns from crystalline PET and PEN fibres.

As there is no evidence of tilt of the *c* axis away from the fibre axis in the mesophase patterns from PET rich samples, but on crystallization from the mesophase all these samples show this type of tilt, it seems reasonable to assume that the tilt occurs when crystallization takes place. It is possible that the tilt occurs as a means of reducing the stress caused by the shape change of the crystal caused by staggering of successive chains being opposed by the surrounding amorphous phase. PEN and PEN rich copolymers (>30% N units) do not show tilts as in PET, however the crystalline PEN based fibre diffraction patterns show distinct streaks between reflections on all the layer lines. Streaking of this kind can arise from faulting in the crystallites parallel to the chain direction, this is demonstrated using optical transforms by Harburn *et al.* [29]. Faulting could also be a means of reducing the stress caused by the sequential shear of chains when register becomes triclinic, as it will compensate for the crystal shape change caused by change in register from smectic A to triclinic. Fig. 14 is a schematic diagram showing how either tilt or faulting would reduce the build up of stress caused by the smectic A mesophase crystallizing into a triclinic structure. The stress relieving mechanism chosen will depend on

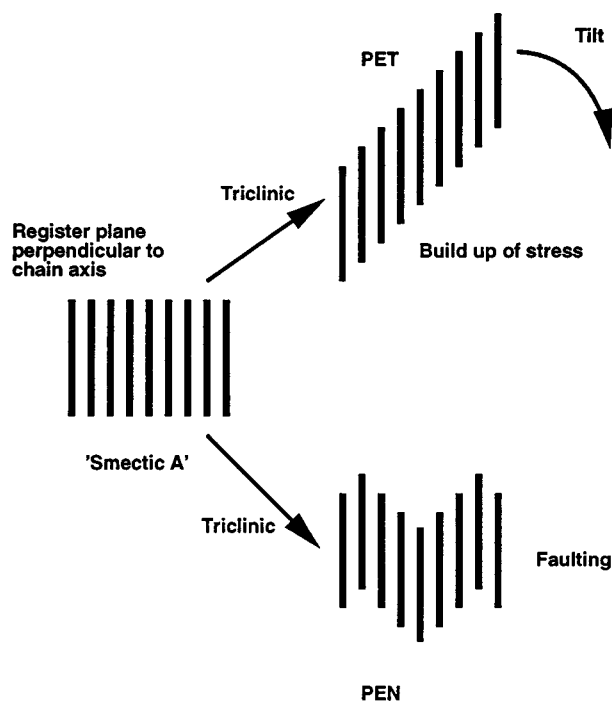


Figure 14 Schematic diagram showing how a co-ordinated c-shear resulting from the mesophase to triclinic crystallization transition could produce oblique crystals, which, on account of the constraint of surrounding material, leads to a tilt of the chain stems away from the fibre axis; or, alternatively, faulting which compensates completely for the obliquity. Experimental evidence suggests that the first mode occurs in PET and those PET/PEN random copolymers which have unit cells based on the PET one (70%–100% T/N), while the second mode, which leads to layer line streaking but no *c* axis tilt, corresponds to what is seen in PEN and PET/PEN random copolymers with crystal structures related to PEN (0–70% T/N).

which of the triclinic cells (PEN or PET) is exhibited by the particular copolymer. Similar proposals to explain the axial tilt of PET fibres have been suggested [13, 15]. In this context, it is worth noting that the copolymers in which the crystal structure is based on the PET structure (70%–100% T) show distinct four-point SAXS diagrams which may be interpreted in terms of oblique crystallites such as envisaged in Fig. 14. The obliquity of the crystallite is of course of the order of 45° against which the ‘fibre tilt’ of a few degrees (depending on composition [9]) is but a small ‘reaction’ to the constraint of the surrounding amorphous phase. Correspondingly, the copolymers based on the PEN structure (0–70% T), show a two point diagram with no evidence of obliquity, but consistent with the c-shear faulting model.

Finally we wish to suggest that in the debate with respect to the presence of a third, ‘oriented amorphous’ phase in PET type polymers, as enjoined for example by Fu *et al.* [30], the possibility of the presence of the orientation induced mesophases, and the possibility that the significant streaking of the reflections on the layer lines in PEN based copolymers (and PEN) can also be interpreted as disorder, should both be borne in mind.

6. Conclusions

As already understood, samples of PET, PEN and their random copolymers, processed and cooled rapidly to avoid crystallization, show stress-induced crystallization during subsequent drawing at temperatures between the glass transition temperature and the crystal melting point.

Samples which are drawn to the point where crystallization has not started or is just beginning, show a transient mesophase which appears to be the precursor of crystallization. This mesophase can be observed by quenching the sample into iced water, where it can be examined at leisure, or by recording the structure at temperature as the sample is being drawn using synchrotron radiation.

The mesophase is apparent from fibre x-ray patterns, its signature being a comparatively weak, yet relatively sharp meridional peak, corresponding to an axial repeat a few percent less than that characteristic of the crystal. This peak is observed in samples in which there is no, or very little, crystallinity as evidenced by the broad but highly oriented equatorial peaks, and the absence of any *hkl* reflections.

The mesophase order is consistent with that of smectic. The lateral width of the main meridional mesophase reflection would suggest that the sequence matching between neighbouring molecules extends laterally over a distance of at least 10 molecule diameters.

Samples in which the mesophase occurs in the absence (or near absence) of crystallinity show no discrete SAXS peaks. However samples which have been crystallised by annealing the mesophase, at constant length, show either two point diagrams or four-point diagrams depending on whether the crystal structure is based on the PET cell (70%–100% T) or the PEN cell (0–70% T).

The two point diagrams for annealed fibres with compositions around 50% T are not especially distinct. The radial (2θ) sharpness of the meridional mesophase reflection corresponds to a crystal thickness which is at least of the same order as the reported long periods of these materials, without taking into account the effect of broadening due to the presence of random sequences of molecules. This observation may also suggest that there is not a two phase microstructure associated with the mesophase state of the fibres.

The absence of oriented SAXS patterns for the highly oriented mesophase samples suggests, either that the mesophase is not associated with any recognisable two-phase structure, or that the densities of the mesophase and a surrounding amorphous phase are too similar to provide the contrast necessary for a clear SAXS pattern (or both !). Further work is necessary to determine which. However, it is worthy of note that in this system there is no SAXS evidence for the mesophase.

The transformation from a smectic A phase to a triclinic crystal structure via a co-ordinated c-shear would cause the mesophase region to change shape. It thus provides a mechanism which can explain the four point SAXS diagram and axial tilt well known for PET and seen [9] also for copolymers with crystal structures based on the PET unit cell (70%–100% T). Similarly, the two point SAXS diagrams together with the absence of tilt in PEN based (0–70% T) structures, are consistent with crystals with no obliquity to the fibre axis. The presence of c-shear faults in such crystals reconciles not only these observations, but also that of significant layer line streaking as well.

Dedication

This paper is dedicated to the memory of Andrew Keller who died last year. Andrew was one of the founding fathers of Polymer Physics, and is famous for his discovery of chain folding in polyethylene crystals. Working with Charles Frank in Bristol University he built up a research school which led the subject over four decades. In a lecture to mark his official retirement in 1991, he drew attention to the importance of mesophases to the mechanism of polymer crystallization citing Oswald's stage rule. Indeed his 'retirement' coincided with a new wind, as he took the understanding of polymer crystallization into new territory, seemingly leaving many established polymer scientists panting to keep up. Of course, Andrew's interest was especially focussed on his beloved polyethylene, and he demonstrated the significance of the hexagonal phase of that polymer, normally only stable under extreme pressure, as a transient mesophase which acted as a precursor to the formation of chain folded crystals. This paper reports a very strident example of a transient mesophase, in the random copolymer system PET/PEN. In this case the mesophase is stabilised by stress, however the Ostwaldian principles are similar, and it appears to act as a precursor to crystallization induced by fibre drawing. Andrew saw these results shortly before he died, but two of us (DJB and AHW) owe much more to him than simply thanks for his encouragement of this particular

piece of work, as he was both teacher and mentor to us throughout most of our professional careers.

References

1. G. E. WELSH, D. J. BLUNDELL and A. WINDLE, *Macromolecules* **31** (1998) 7562.
2. D. J. BLUNDELL, A. MAHENDRASINGAM, C. MARTIN and W. FULLER, *J. Mater. Sci.*, following paper.
3. A. KELLER, in "crystallization of Polymers," edited by M. Dosier (Kluwer) p. 1. NATO Advanced Research Workshop 1992, Mons Belgium.
4. M. IMAI, K. KAJI and T. KANAYA, *Macromolecules* **27** (1994) 7103.
5. A. MAHENDRASINGAM, C. MARTIN, W. FULLER, D. J. BLUNDELL, R. J. OLDMAN, D. H. MACKERRON, J. L. HARVIE and C. RIEKEL, *Polymer* **41** (2000) 1217.
6. N. J. TERRIL, P. A. FAIRCLOUGH, E. TOWNS-ANDREWS, B. U. KOMANSCHEK, R. J. YOUNG and A. J. RYAN, *ibid.* **39** (1998) 2381.
7. P. D. OLMSTED, W. C. K. POON, T. C. B. MCLEISH, N. J. TERRIL and A. J. RYAN, *Phys. Rev. Letters* **81** (1998) 373.
8. A. J. RYAN, P. A. FAIRCLOUGH, N. J. TERRIL, P. D. OLMSTED and W. C. K. POON, *Faraday Disc.* **112** (1999) 13.
9. X. LU and A. H. WINDLE, *Polymer* **36** (1995) 451.
10. *Idem.*, *ibid.* **37** (1996) 2027.
11. S. HANNA, A. ROMO-URIBE and A. H. WINDLE, *Nature* **366** (1993) 546.
12. R. VON BONART, *Kolloid Z. Z.* **213** (1966) 1.
13. *Idem.*, *ibid.* **231** (1968) 16.
14. T. ASANO and T. SETO, *Polymer Journal* **5** (1973) 72.
15. T. ASANO, F. J. BALTA CALLEJA, A. FLORES, M. TANIGAKI, M. F. MINA, C. SAWATARI, H. ITAGAKI, H. TAKAHASHI and I. HATTA, *Polymer* **40** (1999) 6475.
16. F. AURIEMMA, P. CORRADINI, C. DE ROSA, G. GUERRA and V. PETROCCONE, *Macromolecules* **25** (1992) 2490.
17. T. M. NICHOLSON, G. R. DAVIES and I. M. WARD, *Polymer* **35** (1994) 4259.
18. R. JAKEWAYS, J. L. KLEIN and I. M. WARD, *ibid.* **37** (1996) 3761.
19. P. L. CARR, T. M. NICHOLSON and I. M. WARD, *Polym. Adv. Technol.* **8** (1997) 592.
20. S. HANNA and A. H. WINDLE, *Polymer* **29** (1988) 207.
21. A. BISWAS and J. BLACKWELL, *Macromolecules* **21** (1988) 3146.
22. G. E. WELSH and A. H. WINDLE, *Polymer*, submitted.
23. R. D. B. FRASER, T. P. MACRAE, A. MILLAR and R. J. ROWLANDS, *J Appl. Cryst* **9** (1976) 81.
24. D. J. BLUNDELL, D. H. MACKERRON, W. FULLER, A. MAHENDRASINGAM, C. MARTIN, R. J. OLDMAN, R. J. RULE and C. RIEKEL, *Polymer* **37** (1996) 3303.
25. A. MAHENDRASINGAM, C. MARTIN, W. FULLER, D. J. BLUNDELL, R. J. OLDMAN, J. L. HARVIE, D. H. MACKERRON, C. RIEKEL and P. ENGSTROM, *ibid.* **40** (1999) 5553.
26. A. MAHENDRASINGAM, W. FULLER, V. T. FORSYTH, R. J. OLDMAN, D. MACKERRON and D. J. BLUNDELL, *Rev. Sci. Instrum.* **63** (1992) 1087.
27. G. E. WELSH, Ph.D. thesis, Cambridge University, 1998.
28. G. D. BUTZBACH, J. H. WENDORFF and H. J. ZIMMERMANN, *Polymer* **27** (1986) 1337.
29. G. HARBURN, C. A. TAYLOR and T. R. WELBERRY, "Atlas of Optical Transforms" (George Bell, 1975) plate 19.
30. Y. FU, W. R. BUSING, Y. JIN, K. AFFHOLTER and B. WUNDERLICH, *Macromol. Chem. Phys.* **195** (1994) 803.

Received 8 March
and accepted 10 March 2000